Macromolecules
ARTICLE

Macromolecules **2010**, *43*, 7637–7649 **7637**
DOI: 10.1021/ma101336c

PEG−POSS Multiblock Polyurethanes: Synthesis, Characterization, and Hydrogel Formation

Jian Wu,[†,§] Qing Ge,[†,∥] and Patrick T. Mather*[,†,‡,⊥]

[†]*Chemical Engineering Department and Polymer Program, Institute of Materials Science, University of Connecticut, Storrs, Connecticut 06269-3136, and* [‡]*Syracuse Biomaterials Institute & Biomedical and Chemical Engineering Department, Syracuse University, Syracuse, New York 13244.* [§]*Current address: McGowan Institute for Regenerative Medicine, University of Pittsburgh, Pittsburgh, PA 15219.* [∥]*Current address: TyRx Pharma, Inc., Monmouth Junction, NJ 08852.* [⊥]*Current address: Syracuse Biomaterials Institute & Biomedical and Chemical Engineering Department, Syracuse University, Syracuse, NY 13244*

Received June 16, 2010; Revised Manuscript Received August 10, 2010

ABSTRACT: We report the synthesis and characterization of a series of multiblock thermoplastic polyurethane hydrogels synthesized with PEG as the soft segment and incorporating an isobutyl-functionalized POSS diol (TMP POSS diol) in the hard segment. The molecular weight of PEG was systematically varied to include 10, 20, and 35 kg/mol, while the molar ratio of POSS diol (as chain extender) to PEG was varied from 3:1 to 8:1 reported for a polymer series with PEG held constant at 10 kg/mol. The diisocyanate employed for TPU polymerization was 4,4′-methylenebis(phenyl isocyanate) (MDI). Wide-angle X-ray diffraction (WAXD) and small-angle X-ray scattering (SAXS) experiments revealed that both hydrophilic soft segments (PEG) and hydrophobic hard segments (POSS) can form crystalline structures driven by microphase separation due to the thermodynamic incompatibility. Consequently, the POSS nanocrystals serve as physical cross-linking points consisting, themselves, of an inorganic−organic hybrid networks. Interestingly, the polymers swell in water to an extent well-governed by composition, with equilibrium swelling ratio increasing with PEG loading from ∼70% to ∼600%. The water diffusion in the hydrogel was found to be non-Fickian and to depend strongly on PEG crystallinity. The shear modulus of the hybrid hydrogels spanned the range 0.3 MPa $< G <$ 4.0 MPa, a range higher than most hydrogels studied previously. The high stiffness of such thermoplastic hydrogels was found to be controlled by the POSS:PEG mole ratio and was uncorrelated with molecular weight of PEG segment. Given their thermoplastic nature in the dry state, we envision applications involving melt processing of complex shapes and coatings, followed by hydration to hydrogel form.

I. Introduction

Hydrogels are hydrophilic polymer networks with high water absorption capacity. They can absorb from ∼20% up to thousands of times their dry mass.[1] Because of their hydrophilic character and general biocompatibility, hydrogels are used extensively in biology and medicine with applications ranging from delivery systems of bioactive reagents[2−5] (i.e., pharmaceutical drugs, protein, genes, among others), to artificial burns dressing,[6,7] contact lenses,[8−10] tissue engineering scaffolds,[11−14] and water absorption.[15] The importance of hydrogels to biomedical applications can be attributed to several unique characteristics: on one hand, their intrinsic hydrophilicity renders hydrogels impervious to protein adsorption and cell adhesion, while on the other hand, the elastic and soft nature enables them to have low mechanical and frictional irritation when contacted with tissues and organs. Moreover, the high swelling capacity makes them permeable to low molecular weight metabolites while allowing for facile removal residual synthesis reagents by rinsing. Recently, one of the most exciting and increasingly studied applications of hydrogels is their use as matrices for cell delivery in tissue engineering.[16−18] Creating and maintaining the space for the development of new tissues, or even the formation of new organs, provides context that defines the mechanical property requirements of hydrogels. Unfortunately, most hydrogels used commonly today are mechanically weak.[1,19] Recent exceptions to this generalization include the slip-ring hydrogels[20] and hydrogel double networks.[21,22] Nevertheless, the challenge remains for biomaterial scientists to improve and control the mechanical properties of hydrogels applicable to medical devices, drug delivery systems, and tissue engineering.[23−25]

Hydrogels can be cross-linked covalently or physically.[1,3] In the former case, covalent bonds connecting network chains yield a "permanent" hydrogel whose shape is set at the time of gelation and whose mechanical strength is generally low. In order to enhance the mechanical properties, covalently cross-linked hydrogels can be prepared with incorporation of a second, interpenetrating, polymer network with covalent cross-linking.[26,27] By comparison, physically cross-linked hydrogels (also called "reversible" hydrogels) feature a network structure consisting of molecular entanglements and/or secondary forces, such as ionic interactions, hydrogen bonding, hydrophobic interaction, and protein self-assembly via α-helices that specifically interact with each other.[28,29] In contrast to the covalent networks, physical networks offer the advantages of being reversible, easily handled, injectable, and thermally processable by such methods as extrusion, injection molding, or thermoforming. Such features render physically cross-linked hydrogels more attractive for large-scale production.

Poly(ethylene glycol) (PEG), a water-soluble polymer incorporated in the present work, is one of the most widely investigated

*Corresponding author: e-mail ptmather@syr.edu, Tel 1-315-443-8760, Fax 1-315-443-4936.

Published on Web 08/17/2010

building blocks used in hydrogels with desired properties in the biotechnology and biomedical applications.[30−37] Because of its resistance to adsorption of polymers in aqueous environments, PEG-based hydrogels and surfaces with grafted PEG brushes feature protein rejection, nonimmunogenicity, antithrombogenicity, and nonantigenicity. Although PEG may interact with cell membranes, it does not harm living cells or proteins and is generally nontoxic. PEG-based hydrogels can be obtained through the formation of covalent networks using free radical polymerization of α,ω-functionalized diacrylate- or dimethacrylate-terminated PEG or, more recently, through thiol−ene network formation.[31,38,39] Alternatively, PEG can be physically cross-linked through the entanglement of PEG chains (possible at high molecular weight) or intermolecular complexation by hydrogen bonds between PEG and other polymers, such as poly(methacrylic acid) (PMAA).[40] Moreover, PEG can be served as a physically cross-linked soft segment in a multiblock polyurethane (PU) structure.[41,42] Indeed, this paper develops such methods, using strongly hydrophobic POSS in the "hard segment" of the TPU.

Polyhedral oligosilsesquioxanes (POSS) are a family of hybrid molecules consisting of a cagelike inorganic (silicon−oxygen) core and eight variable organic vertex groups.[43] In monomer form, POSS molecules crystallize as spheres within a rhombohedral (or hexagonal) lattice with well-defined melting points that depend on the vertex group. Commonly, such vertex groups are linear or cyclic aliphatic molecules, engendering strong hydrophobicity to the POSS molecule. Depending on their compatibility with the polymer matrix, POSS moieties can either disperse nearly within a molecular level or aggregate into nanoscale domains.[44,45]

We anticipated that hydrophobic POSS macromers would aggregate and crystallize to form nanoscale crystals when polymerized with hydrophilic PEG, considering expected microphase separation associated with thermodynamic incompatibility between hydrophilic PEG and hydrophobic POSS. Such POSS crystals would become the physical cross-links of a unique hybrid hydrogel. We further expected POSS moieties reinforce the resultant hydrogels at the nanoscale, possibly yielding desirable mechanical properties. Considering further that hydrogel elasticity depends strongly on the molecular weight between cross-links, M_c, and thus swelling degree, we sought to control swelling behavior through the POSS content (wt %) and PEG molecular weight.

Previously, we reported on the synthesis of PEG telechelics that incorporate one polyhedral oligosilsesquioxane (POSS) moiety at each end of the PEG chain through formation of a urethane bond.[46−48] Similarly, Zeng et al.[49] incorporated POSS-end-capped PEG telechelics into chemically cross-linking poly(*N*-isopropylacrylamide) (PNIPAAm) networks to form physical interpenetrating polymer networks (IPNs). The resulting organic−inorganic hydrogels featured much faster thermoresponse than their PNIPAAm counterparts. More recently, click chemistry has been applied to achieve similar structures.[50] Here, we extend this POSS−PEG−POSS telechelic architecture to PEG multiblock thermoplastic polyurethanes by incorporating POSS to form a hybrid hydrogel with good mechanical properties associated with the multiblock architecture. We note that a recent report from us utilizes the same materials for the preparation and study of antimicrobial hydrogel webs processed by electrospinning.[51] In this paper, we report on the synthesis and characterization of the hybrid PEG−POSS polyurethanes. The molecular weight of PEG and the POSS:PEG molar ratio of POSS:PEG were systematically varied, and the resulting water absorption and mechanical properties were measured. Such variations enabled good control over hydrogel properties, most notably the degree of water swelling and the hydrogel elastic shear modulus.

II. Experimental Methods

1. Sample Preparation. Hybrid thermoplastic polyurethanes (TPUs) were synthesized to contain poly(ethylene glycol) (PEG) soft segments with hard segments consisting of 2,2,4-trimethyl-1,3-pentane (TMP) POSS diol (R-group = isobutyl, ^{i}Bu), hereafter "POSS diol", and 4,4′-methylene bis(phenyl isocyanate) (MDI), as shown in Scheme 1. A one-step method was used to synthesize the TPUs. Before each reaction, PEG (Fluka) with selected molecular weight was purified by dissolving in THF and reprecipitating in *n*-hexane. The resulted powder was then filtered and dried in a vacuum oven at room temperature overnight. POSS-diol (99.5%, Hybrid Plastics) and MDI (98%, Aldrich) were used without further purification. In a 100 mL three-neck flask, POSS-diol and PEG with prescribed molar ratio were dissolved in toluene (Fisher, ACS Certified), which had been dried over molecular sieves (4 Å, Aldrich). Under the protection of gaseous nitrogen purge, the flask was heated to 50 °C and a stoichiometric amount of MDI was added into the 10 wt % toluene solution. The reaction mixture was further heated up to 90 °C, and several drops of dibutyltin dilaurate were added through a syringe. The reaction was kept at 90 °C for 3 h under a nitrogen atmosphere, and a significant increase in viscosity was observed. The resulting toluene solution was then precipitated into an excess amount of *n*-hexane, filtered, and washed with deionized water several times in order to remove any unreacted POSS-diol and PEG. The obtained products were then dried and redissolved in toluene and poured into casting dishes, where the solvent evaporated to yield semitransparent, mechanically robust films with prescribed thickness of ∼0.5 mm.

We have adopted a nomenclature to distinguish samples by composition: PEG(α)POSS$_\beta$, where α is the molecular weight of PEG in the unit of kg/mol and β is the molar ratio of POSS-diol to PEG. For instance, PEG(10)POSS$_3$ is a hybrid thermoplastic polyurethane synthesized from PEG with molecular weight of 10 kg/mol, and TMP POSS-diol is a macromer whose molar ratio to PEG is 3:1.

2. Molecular Characterization. The molecular weight and molecular weight distribution of the polyurethanes were determined by gel permeation chromatography (GPC) (Waters Associates, 150-C plus) with a PL-ELS 1000 control detector (Polymer Laboratories). The samples, dissolved in THF with concentration of ∼0.1 wt %, were filtered and injected at 35 °C using THF as mobile phase and at a flow rate of 1 mL/min. GPC data reported for the molecular weights and molecular weight distributions are relative to a calibration based on monodispersed polystyrene standards (Polymer Standards Service-USA, Inc.).

To identify the chemical structures of the polyurethanes, FT-IR spectra were obtained by using a Nicolet MAGNA-IR 560 spectrometer at room temperature. The samples were neat thin coatings cast from THF solutions (5 wt %) upon KBr windows. The coated KBr window was dried under vacuum at room temperature for several minutes, and special care was taken to avoid moisture before measurements. To further determine the actual ratio of POSS to PEG in the products, ^{1}H NMR spectra of the samples were obtained by employing a Bruker 500 MHz DMX500 high-resolution spectrometer. Samples were made from $CDCl_3$ solutions and run at room temperature.

3. Microstructural Characterization. Wide-angle X-ray diffraction (WAXD) was performed to detect the microstructure of TPU films with varying POSS:PEG molar ratio and PEG homopolymer molecular weight. Measurements were conducted at room temperature on a Bruker D5005 X-ray diffractometer operated at 40 kV and 40 mA with Cu Kα radiation (wavelength, λ = 1.5418 Å). The microphase separation was further characterized by small-angle X-ray scattering (SAXS) experiments conducted on a Bruker SAXS instrument equipped with a Ni filter, pinhole collimation, and a Histar area detector. Here, the X-ray source was also Cu Kα radiation, but obtained

Scheme 1. Synthetic Scheme for the Preparation of the Hybrid Thermoplastic Polyurethanes Yielded through Condensation Reaction between 4,4′-Methylenebis(phenyl isocyanate) (MDI) and Both of PEG and Isobutyl-Functionalized POSS-diol[a]

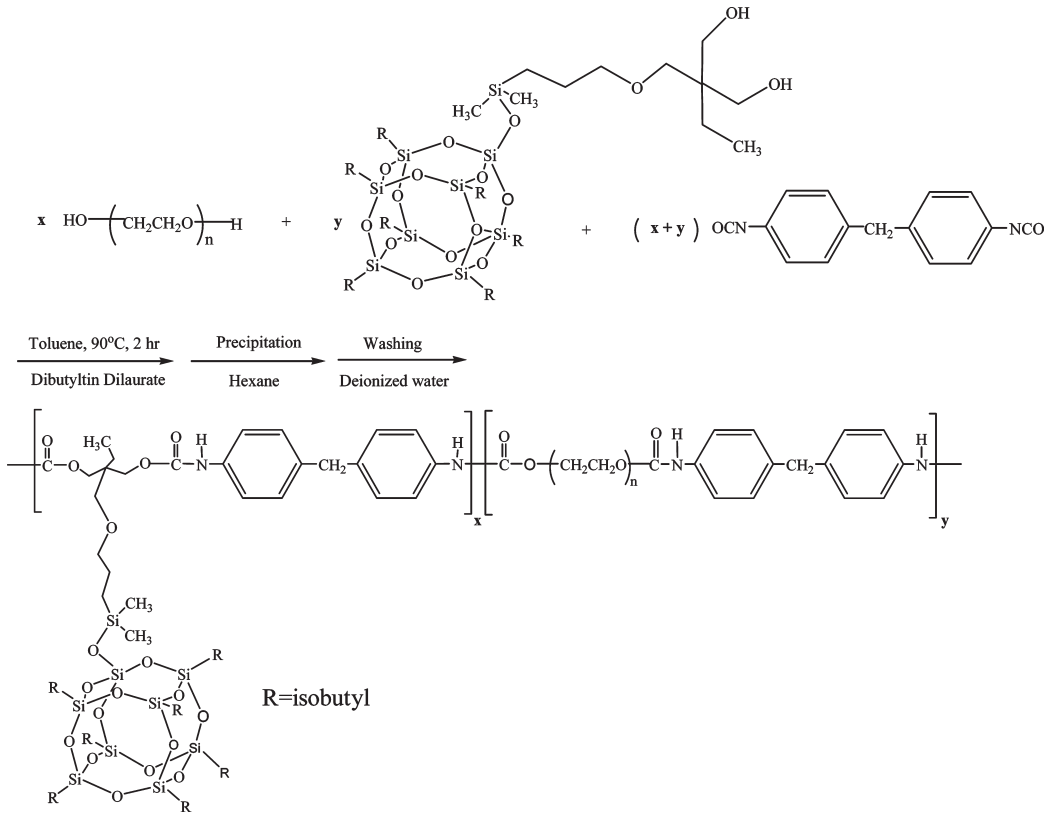

[a] The reaction was conducted at 90 °C in toluene, and the catalyst was dibutyltin dilaurate.

from Rigaku rotating anode operated at 40 kV and 100 mA. The distance between sample and detector was fixed at 108 cm, and the yielded scattering angle (θ) ranged from 0.5° to 5.0°, allowing d-spacing from 17.7 to 1.8 nm to be observed. Each SAXS profile was corrected by background subtraction, with the background consisting of the detector profile obtained for an empty chamber but same exposure time.

Scanning electron microscopy (SEM) was employed to investigate the morphology of the hydrogels obtained from the hybrid thermoplastic polyurethanes by using a Philips XL30 Environmental SEM system at an accelerating voltage of 15 kV. Before SEM imaging, the hybrid hydrogel samples were desiccated in a freeze−dry system (Freezone 4.5, Labconco, Kansas City, MO), in an attempt to preserve the hydrogel structure in the swollen state, and then sputter-coated with a thin layer of gold using a DENTON VACUUM-DESK II gold sputter coater.

4. Thermal Analysis. The melting behavior of the POSS hard block and PEG soft block in the thermoplastic hybrid polyurethanes was investigated by DSC (DSC2920, TA Instruments) equipped with a mechanical intercooler (for cooling to −60 °C) under a continuous nitrogen purge (50 mL/min) using the procedure described below: after annealing each sample at 150 °C for 5 min to melt the residual POSS crystals, the samples (5−10 mg) were cooled to −50 °C with a ramping rate of −10 °C/min and then heated up to 150 °C with a ramping rate of 10 °C/min. We examined, in this manner, the dependence of melting enthalpy (heat of fusion) and melting point of POSS and PEG on composition and molecular weight of PEG.

5. Swelling Measurements. The water-swelling behavior of the hybrid polyurethanes was studied by a gravimetric procedure. Each dry film sample was immersed in doubly distilled water at room temperature. The water-swollen samples were removed from the bath at prescribed time points, gently pressed between two pieces of filter paper to remove any excess water on the surface, and weighed by an electronic analytical balance (XS240, Mettler Toledo Inc.) with an accuracy of $\pm 10^{-4}$ g. The swelling ratio (S) was quantified using the equation

$$S\,(\%) = \frac{m_t - m_d}{m_d} \times 100 \qquad (1)$$

where m_t and m_d are the mass of swollen and dried samples, respectively. The equilibrium swelling ratio (S_{eq}) was determined after the hydrogel was immersed in water for 2 days, a swelling time separately determined to yield equilibrium swelling.

6. Mechanical Properties. Temperature-dependent mechanical properties of the hybrid polyurethanes were measured using dynamic mechanical analysis (DMA2980, TA Instruments) in tensile mode at an oscillation frequency of 1 Hz. 0.010 N of static force was used, and the displacement amplitude of oscillation was 20 μm (or 0.125% of the tensile strain). The automatic tension mode was used with the static stress maintained at 110% of the magnitude of the dynamic stress. After allowing thermal equilibration at −50 °C for 5 min, the samples were heated up from −50 to 150 °C with a ramping rate of 2 °C/min. The typical dimensions of the as-cast film are 16 mm × 2 mm × 0.5 mm (length × width × thickness).

The shear modulus of the equilibrium hydrogels was measured by using the ARES rheometer (Advanced Rheometric Expansion System, TA Instruments, Inc.) with a serrated parallel plate accessory (25 mm in diameter). In order to avoid the moisture loss during the experiment, the sample edge was carefully sealed by poly(dimethylsiloxane) (PDMS) with low viscosity (viscosity = 1 Pa·s at 25 °C, Scientific Polymer Products, Inc.). In particular, the dynamic shear moduli were measured over the frequency range $0.1 < \omega < 100$ rad/s at 25 °C for all of the samples. The existence and extent of the linear viscoelastic regime were determined by measuring the dynamic shear storage

Table 1. Molecular Characterization of the Hybrid Thermoplastic Polyurethanes

sample	POSS:PEG (feed ratio)	POSS:PEG[a] (actual ratio)	M_w (kg/mol)[b]	M_w/M_n[b]	wt % POSS[a]
PEG(10)POSS$_3$	3:1	2.8:1	47.4	1.42	26.2
PEG(10)POSS$_4$	4:1	4.1:1	48.0	1.44	34.2
PEG(10)POSS$_6$	6:1	6.2:1	54.2	1.54	44.0
PEG(10)POSS$_8$	8:1	8.0:1	49.2	1.30	50.5
PEG(20)POSS$_{16}$	16:1	16.9:1	79.8	1.45	52.0
PEG(35)POSS$_{28}$	28:1	28.3:1	66.0	1.24	51.1

[a] Determined by ^{1}H NMR. [b] Determined by GPC.

and loss moduli, $G'(\omega)$ and $G''(\omega)$, as a functions of strain ($0.1 < \gamma < 1.0\%$) at an angular frequency of 6.28 rad/s. All of the measurements were carried out within the linear viscoelastic range, where $G'(\omega)$ and $G''(\omega)$ are independent of strain.

III. Results and Discussion

1. Synthesis. The synthesis of PEG-based multiblock hybrid thermoplastic polyurethanes incorporating POSS is shown schematically in Scheme 1 and follows the methodology previously reported for other POSS-containing polyurethanes.[46,52] The urethane linkages were formed through the addition reaction between isocyanate groups of the 4,4-methylenebis(phenyl isocyanate) (MDI) and the hydroxyl groups of either poly(ethylene glycol) (PEG) or POSS diol. Because of their different glass transition temperatures and melting points, the chemically distinct blocks of the multiblock polyurethane can be regarded as "soft" segments (PEG-based) and "hard" segments (POSS-based). It is known that PEG is a broadly soluble polymer, including water solubility, while the POSS macromer and POSS-containing polymers will generally only dissolve in the organic solvents, such as tetrahydrofuran, chloroform, or hexane. In light of this solubility contrast, PEG-segments and POSS-segments can contribute to the hydrophilic network and hydrophobic cross-links, respectively. Thus, in our multiblock polyurethanes, two variables exist for tuning the final properties of the resulting hydrogels: (i) molecular weight (MW) of PEG homopolymer and (ii) the molar ratio between POSS and PEG (or weight fraction of POSS and PEG segments in the TPUs). Here, we varied the molecular weights of PEG homopolymers to include 10, 20, and 35 kg/mol in the syntheses. We chose PEG homopolymers whose molecular weights were larger than the PEG entanglement molecular weight ($M_e \cong 4400$ g/mol)[53] to engender molecular entanglements that may enhance mechanical properties of the final hydrogels. The hydrophilic−hydrophobic balance can be controlled with the variation of POSS weight fraction. For those samples prepared from PEG with molecular weight of 10 kg/mol, the molar ratio of POSS to PEG was varied to include 3:1, 4:1, 6:1, and 8:1. This results in a range of POSS-segment weight fractions spanning 28−50 wt %. In another series of compositions, the POSS incorporation level was held fixed at 50 wt % while the PEG molecular weight was varied, as mentioned above. Characterization of both series was designed to reveal the dependences of swelling behavior and mechanical properties on the POSS-based hard segments and PEG molecular weight.

The molecular weights and molecular weight distributions of the hybrid polyurethanes determined by GPC (Supporting Information Figure 1), along with sample nomenclature definitions, are detailed in Table 1. The molecular weight of the yielded products spanned the range of 47 kg/mol $< M_w <$ 80 kg/mol, and their corresponding molecular weight polydispersities (following precipitation) varied from 1.3 to 1.6, which are relatively narrow for step-growth polymerizations. The chemical structures of the polyurethanes were identified by FT-IR and ^{1}H NMR. FT-IR spectra of reactants (Supporting Information Figure 2) reveal a strong absorption band at 2290 cm^{-1} ascribed to C═N (nitrile) stretch in the isocyanate group (−N═C═O) and a very weak broad absorption band of the end hydroxyl group (−OH) of PEG homopolymer at 3400−3500 cm^{-1} due to its low hydroxyl group density (the broadness can also be due to hydrogen bonding). By comparison, POSS-diol featured a stronger absorption band of hydroxyl group (−OH) of POSS-diol macromer centered at 3400 cm^{-1}, probably due to its higher hydroxyl group density and lack of hydrogen bonding, and a strong band at 1110 cm^{-1} assigned to the stretching vibration of Si−O−Si groups in the silsesquioxane cages. For the case of the hybrid polyurethane, the characteristic absorption bands of both isocyanate group (2290 cm^{-1}) in MDI and hydroxyl group in PEG and POSS-diol completely disappeared. Instead, two new characteristic peaks appeared: one centered at 3310 cm^{-1}, attributed to N−H stretching within urethane linkages, and the other is centered at 1720 cm^{-1}, attributed to the typical stretching of ester carbonyl groups (C═O) within the urethane linkages. Thus, the isocyanate groups of MDI successfully reacted with hydroxyl group (3400 cm^{-1}) in PEG and POSS-diol to form urethane groups (−NH−CO−O−). Meanwhile, we also observed strong absorption bands in the range of 2800−3000 cm^{-1} ascribed to the asymmetric and symmetric C−H stretching vibrations. The peak centered at 1530 cm^{-1} is in-plane bending of N−H bonds. From 1000 to 1200 cm^{-1}, there are strong C−O and Si−O stretching vibrations: the peak centered at 1110 cm^{-1} is the typical vibration band of –Si−O−Si–, and the absorption band at 1115 cm^{-1} is attributed to characteristic –C−O−C— stretching vibration of the repeated $-O-CH_2-CH_2-$ units of the PEG backbone. Finally, we observed characteristic bands of the crystalline phase of PEG centered at 963 and 843 cm^{-1}.[54]

The characteristic proton signals in ^{1}H NMR spectrum (Supporting Information Figure 3) of the hybrid polyurethane (PEG of 10 kg/mol, POSS:PEG = 8:1) in $CDCl_3$ are as follows: δ 7.07 ppm (benzene ring, −C*H*−), δ 4.1 ppm (−O−CO−N*H*−), δ 3.88 ppm (Ar−CH_2−Ar), δ 3.64 ppm (PEG, −CH_2−CH_2−O−), δ 3.42 ppm (−CO−O−CH_2−), δ 3.32 ppm (−CH_2−O−CH_2−), δ 1.85 ppm (isobutyl group, −CH$_2$−C*H*(CH$_3$)$_2$), δ 1.58 ppm (−O−Si(CH$_3$)$_2$−CH$_2$−CH_2−CH$_2$−O−), δ 1.26 ppm (C(CH$_2$)$_3$−CH_2−CH$_3$), δ 0.95 ppm (isobutyl group, −CH$_2$−CH(CH_3)$_2$), δ 0.89 ppm (C(CH$_2$)$_3$−CH$_2$−CH_3), δ 0.60 ppm (isobutyl group, −CH_2−CH(CH$_3$)$_2$ and −O−Si(CH$_3$)$_2$−CH_2−), and δ 0.12 ppm (−O−Si(CH_3)$_2$−CH$_2$−). The emergence of a proton signal at 4.14 ppm evidenced the formation of urethane group (−O−CO−NH−),[46] which matches our observation in the FT-IR spectrum. Besides the identification of chemical structures, the ^{1}H NMR spectrum can also be used to quantitatively determine the content of POSS incorporated in the hybrid polyurethanes. In particular, the molar ratio of POSS to PEG can be obtained by comparing ratio of the integration value of the proton resonance at δ 0.12 ppm (−O−Si(CH_3)$_2$−CH$_2$−) for POSS macromers to that at δ 3.64 ppm (PEG, −CH_2−CH_2−O−). Before comparison, both of the integration values

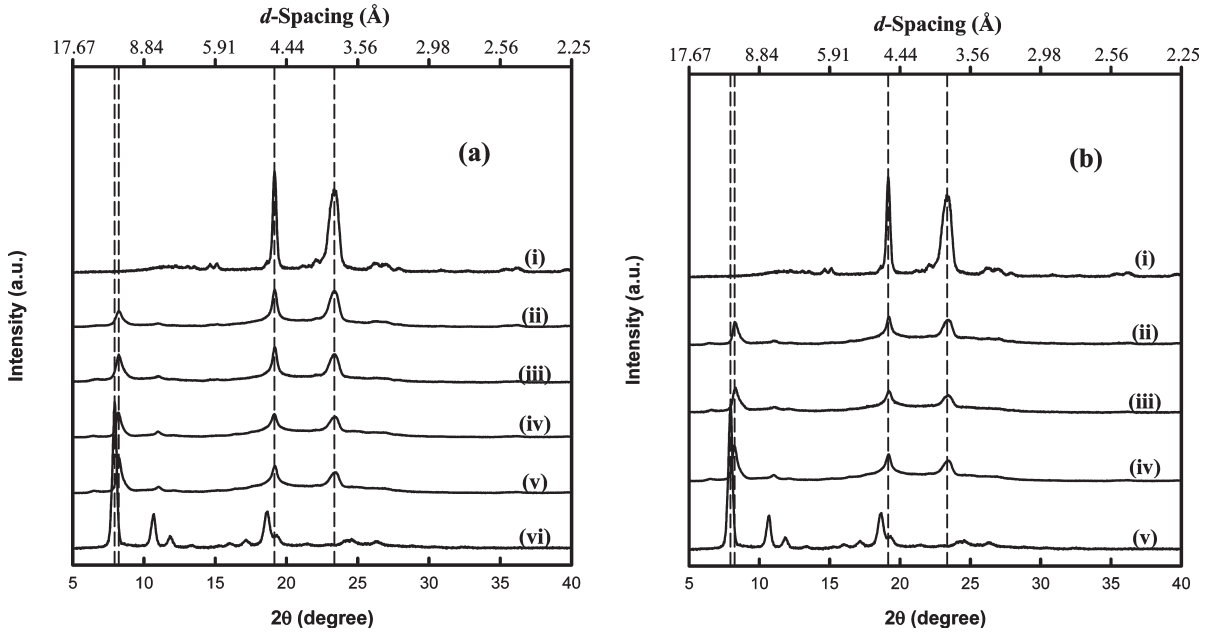

Figure 1. WAXD patterns of the hybrid polyurethanes from PEG and TMP POSS-diol macromers indicated in Table 1. The molar ratio of POSS to PEG (10 kg/mol) is varied in (a): (i) PEG homopolymer, 10 kg/mol, (ii) POSS:PEG = 3:1, (iii) POSS:PEG = 4:1, (iv) POSS:PEG = 6:1, (v) POSS:PEG = 8:1, and (vi) pure POSS-diol. The effect of molecular weight of PEG homopolymers is shown in (b), where weight fraction of POSS segment is maintained at ~50 wt %: (i) PEG homopolymer, 10 kg/mol, (ii) TPU with PEG of 35 kg/mol, (iii) TPU with PEG of 20 kg/mol, (iv) TPU with PEG of 10 kg/mol, and (v) pure POSS-diol. The X-ray wavelength (λ) is 1.5418 Å.

were normalized to those for a single proton. The molar ratios of POSS to PEG, measured in this way, and the resulting POSS-segment weight fraction in the hybrid polyurethanes are listed in Table 1. Good agreement between prescribed and resultant compositions was obtained.

2. Microstructural Characterization. Wide-angle X-ray diffraction (WAXD) patterns of the novel hybrid thermoplastic polyurethanes are shown in Figure 1a,b, revealing the dependences of microstructure on POSS content and PEG molecular weight, respectively. Compared with WAXD patterns of pure PEG and TMP POSS-diol, there are three characteristic diffraction peaks in polyurethane samples. The two diffraction peaks centered at *d*-spacing of 4.6 Å (2θ = 19.2°) and 3.8 Å (2θ = 23.4°) are attributed to the 120 and $1\bar{3}2$ reflections of PEG monoclinic unit cell,[55−57] respectively. A third peak at a *d*-spacing of 10.7 Å (2θ = 8.2°) is attributed to 101 reflection peak of POSS rhombohedral unit cell, although it is a little smaller than the reflection peak of TMP POSS-diol at *d*-spacing of 11.1 Å (2θ = 7.9°). Clearly, the hydrophilic segment of PEG and hydrophobic POSS can each form independent crystalline microstructures, indicating microphase separation that we attribute to thermodynamic incompatibility. The diffraction peaks of PEG crystals in polyurethane occur at the same 2θ angles as for pure PEG, indicating that only PEG is involved in crystals of PEG-rich domains. By comparison, the *d*-spacing of POSS crystals in polyurethane is smaller than that of pure POSS−diol, indicating that POSS moieties alone (not MDI units) compactly stack into a crystalline structure—possibly a 2D raft structure[44] (discussed below)—and that this structure is different from that of the POSS-diol molecule that forms 3-D POSS crystals. As shown in Figure 1a, with the increase of POSS content (ii → v), the diffraction intensity of reflection peaks for PEG crystals decreases while those related to reflection from POSS crystal planes increase and sharpen. However, comparison of polymers with the same POSS wt % (Figure 1b, ii−iv) reveals nearly identical microstructure with WAXD profiles nearly independent of the PEG molecular weight.

The high contrast in electronic densities between PEG-rich phase and POSS-rich phase makes it possible for us to further explore the microstructures in the hybrid polyurethane due to the microphase separation employing small-angle X-ray scattering (SAXS), with which unoriented halos were observed. The profiles of scattering intensity as a function of scattering angle are presented in Figure 2a,b, showing patterns of varying POSS content and PEG molecular weight, respectively. The scattering vector profile of each polyurethane sample features a characteristic scattering peak. As is well-known, the relationship between scattering vector (q) and scattering angle (θ) is expressed as follows:

$$q = \frac{4\pi}{\lambda}\sin\left(\frac{\theta}{2}\right) \tag{2}$$

where λ is the X-ray wavelength (Cu Kα = 1.5418 Å). The average distance (d) between domains can be estimated by the peak position using the simple equation as follows:

$$d = \frac{2\pi}{q_{\max}} \tag{3}$$

where $q_{\max}$ is characteristic scattering vector corresponding to the maximum SAXS intensity and where a "domain" is a characteristic compositional fluctuation within the multiblock copolymers.

We observed that the domain size is nearly independent of POSS content and molecular weight of PEG, consistently defined between 2.5 and 2.7 nm. If this domain size is that of POSS nanocrystals, it is just double the size of an individual POSS molecule, consistent with the double-layer "raft" model of POSS crystallization put forth by Coughlin et al.[58,59] Combined, our WAXS and SAXS observations indicate that hydrophilic PEG blocks and hydrophobic segments separately crystallize, indicating either microphase separation driven by thermodynamic incompatibility or crystallization-induced microphase separation. Thermal analysis (discussed below) supports the former hypothesis, but SAXS

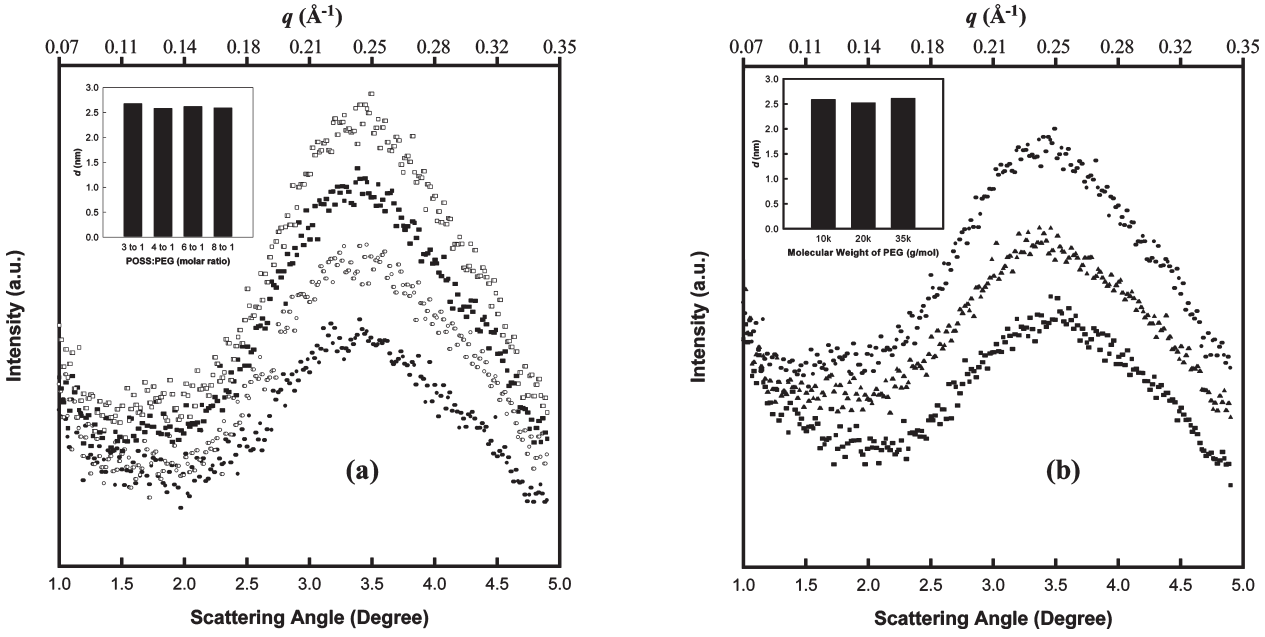

Figure 2. Background-corrected SAXS intensity as a function of scattering angle for the hybrid polyurethanes from PEG and TMP POSS-diol macromers indicated in Table 1. The molar ratio dependence between POSS and PEG of 10 kg/mol is presented in (a): (●)POSS:PEG = 3:1, (○) POSS:PEG = 4:1, (■) POSS:PEG = 6:1, and (□) POSS:PEG = 8:1. The effect of molecular weight of PEG homopolymers is shown in (b), where weight fraction of POSS segment is ~50 wt %: (●) TPU with PEG of 10 kg/mol, (■) TPU with PEG of 20 kg/mol, (▲) TPU with PEG of 35 kg/mol. The X-ray wavelength (λ) is 1.5418 Å. Insets: relative average distance ($d = 2\pi/q_{max}$) between domains as a function of (a) molar ratio of POSS to PEG and (b) molecular weight of PEG.

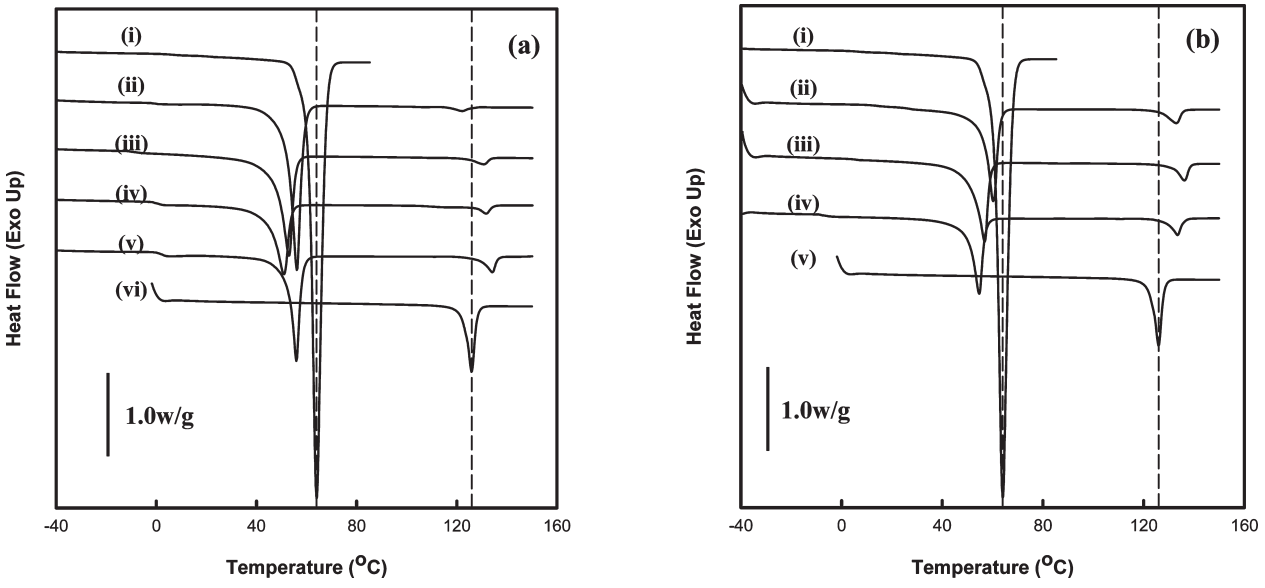

Figure 3. Differential scanning calorimetry (DSC) analysis of the hybrid polyurethanes from PEG and TMP POSS-diol macromers listed in Table 1. The molar ratio dependence between POSS and PEG of 10 kg/mol is presented in (a): (i) PEG homopolymer, 10 kg/mol, (ii) POSS:PEG = 3:1, (iii) POSS:PEG = 4:1, (iv) POSS:PEG = 6:1, (v) POSS:PEG = 8:1, and (vi) pure POSS-diol. The effect of molecular weight of PEG homopolymers is shown in (b), where weight fraction of POSS segment is ~50 wt %: (i) PEG homopolymer, 10 kg/mol, (ii) TPU with PEG of 10 kg/mol, (iii) TPU with PEG of 20 kg/mol, (iv) TPU with PEG of 35 kg/mol, and (v) pure POSS-diol. The DSC trace curves recorded the second heating with ramping rate of 10 °C/min. The dashed lines were referred for melting temperatures of pure PEG and POSS-diol.

analysis at elevated temperatures will be required to prove this definitively.

3. Phase Behavior. The phase behavior of the PEG−POSS hybrid polyurethanes was investigated using DSC analysis. Figure 3a,b shows the DSC heating traces for all of our samples, while glass transition temperatures, melting points, and latent heats of melting are summarized in Table 2. Figure 3a presents a series of polyurethane samples prepared from PEG diol with a molecular weight of 10 kg/mol and with variation in POSS:PEG molar ratio from 3:1 to 8:1 (and corresponding POSS wt % increasing from 26% to 50%). Two characteristic melting peaks are evident. In light of the behavior of pure PEG and POSS-diol samples (traces i and vi, respectively), the lower melting point in the range from 50 to 60 °C is attributed to the PEG-rich soft block, while the higher one ranging from 120 to 135 °C is attributed to the POSS-rich hard block. With increasing POSS:PEG molar ratio, the melting peak of the POSS-rich phase sharpens and shifts from 122.2 to 134.3 °C—higher than T_m for the 3D POSS crystal, 124.2 °C. The corresponding latent heat of

Table 2. Summary of Thermal Transitions for the PEG−POSS TPUs Evaluated Using DSC

sample	POSS:PEG (feed ratio)	T_g (°C)	ΔH_m^{PEG} (J/g)	T_m^{PEG} (°C)	ΔH_m^{POSS} (J/g)	T_m^{POSS} (°C)
PEG(10)$POSS_3$	3:1	−1.78	82.92	56.1	2.80	122.2
PEG(10)$POSS_4$	4:1	−8.87	57.87	52.9	4.25	130.9
PEG(10)$POSS_6$	6:1	0.48	45.68	51.1	6.64	131.7
PEG(10)$POSS_8$	8:1	1.85	47.03	55.9	7.86	134.3
PEG(20)$POSS_{16}$	16:1	4.84	48.50	56.8	7.90	136.3
PEG(35)$POSS_{28}$	28:1	13.20	49.06	60.4	7.92	132.9
PEG(10)			185.0	64.6		
POSS-diol					25.24	124.2

melting also *increased* from 2.80 J/g to 7.86 J/g. On the contrary, the melting peak related to PEG segments broadened and *decreased* from 56.1 °C (3:1) to 51.1 °C (6:1). The corresponding latent heat of melting for the PEG-rich phase decreased from 82.92 J/g (3:1) to 45.68 J/g (6:1). Here, the reference masses for the latent heats measured were those for the entire multiblock copolymer. Considering the microphase-separated structure, the size and perfection of crystals are dependent on the volume fraction of each crystallizable component. At fixed PEG molecular weight, as the POSS:PEG molar ratio increases, the POSS weight fraction increases while the PEG wt % decreases. Consequently, the melting temperature of POSS-segments was expected to increase and sharpen.

Meanwhile, the melting peak of PEG-segments should decrease and possibly broaden. However, we surprisingly found when POSS:PEG molar ratio was increased to 8:1, the melting peak and melting enthalpy of PEG-segments *increased* stepwise to 55.9 °C and 47.03 J/g, respectively. This may be due to a distinct change in multiblock copolymer morphology with the increase of POSS:PEG ratio to a value corresponding to a weight percentage near 50%. Ignoring a slight density difference, the 8:1 sample features ~50 vol % for each phase, likely leading to a lamellar phase or a cocontinuous microstructure with the distinct thermal properties measured. More extensive SAXS measurements complemented by TEM are needed to prove this postulation.

The PEG molecular weight of the TPUs impacts phase behavior significantly. Figure 3b shows the dependence of melting behavior on the molecular weight of the PEG incorporated into the polyurethanes, maintaining the POSS content fixed at 50 wt %. We observed that the PEG-based melting point increased with PEG molecular weight, while the latent heat of melting for the same phase remained essentially constant. Not surprisingly, the melting enthalpy of POSS segments is nearly constant and unaffected by PEG molecular weight for this series, whereas the melting transition of POSS segments shows the complex dependence of PEG molecular weight. Compared with the PEG blocks with 10 and 35 kg/mol, the hybrid hydrogels obtained from PEG of 20 kg/mol feature a little higher melting temperature. Unfortunately, we cannot provide a rational explanation to this observation so far.

The glass transition temperatures (T_gs) of the hybrid TPUs were determined using DSC, the results being summarized in Table 2. It was found that the glass transition temperatures have a close relationship with the level of POSS loading and molecular weight of PEG diol. For those TPUs with PEG held constant at 10 kg/mol, T_g increased modestly with POSS loading from −8.9 to 1.9 °C (one exception was PEG(10)$POSS_3$). Xu et al.[60,61] investigated the T_g enhancement mechanism of POSS-based hybrid polymers employing FT-IR spectra and reported that a strong interaction between POSS siloxane and the polar carbonyl group contributes to a significant T_g increase. In good agreement with their observations, we also found that, for instance, the FT-IR spectrum of PEG(10)$POSS_8$ exhibited a shoulder peak centered at 1072 cm^{-1} (as indicated in Supporting Information Figure 4). In our case, the polar groups, which induce the dipole−dipole interaction with POSS siloxane, could be the carbonyl group and/or ether group of the TPU backbone. Because of the microphase-separated microstructure, this dipole−dipole interaction might mainly take place at the interface between the POSS-rich phase and the PEG-rich phase. This increase in T_g with POSS loading, despite the microphase-separated microstructure, indicates an interfacial effect wherein the rigid POSS-rich phase decreases segmental flexibility of the adjacent PEG-rich phase, leading to the T_g enhancement. The exception of PEG(10)$POSS_3$ may be due to the high crystallinity of PEG-rich domains for that sample. The glass transition temperature for pure PEG-diol was not determined from by DSC due to the fact that T_g of highly crystalline PEG is −66.7 °C (206.5 K),[62] which was out of our experimental temperature range examined. By comparison, T_g increased from 1.9 to 13.2 °C with increasing molecular weight of PEG from 10 to 35 kg/mol with POSS incorporation level held constant at 50 wt %. We attribute this finding to a simple molecular weight effect commonly observed in polymers.

Dynamic mechanical analysis (DMA) was employed to characterize the temperature-dependent linear viscoelastic properties of the hybrid polyurethanes. The tensile storage modulus and loss tangent (tan δ) traces for all of the compositions are shown in Figure 4a,b, revealing the dependences on POSS content and PEG molecular weight, respectively. In Figure 4a, we observe two broad loss tangent peaks and the start of a third with increasing temperature. One loss tangent peak is located in the temperature range $0 < T < 20$ °C that, by comparison with the DSC results, we attribute to a glass transition event. With increasing POSS:PEG molar ratio, this tan δ peak shifts to higher temperature, indicating an increasing impact of the POSS-moieties on chain flexibility. Another loss tangent peak appears in the higher temperature range, $50 < T < 60$ °C, and is attributed to the melting of PEG-segment crystals. On crossing the melting point of PEG moieties, the hybrid polyurethanes exhibit a stepwise decrease in tensile storage modulus. The magnitude of this stepwise decrease, itself, decreases from 430 to 170 MPa with the increase of POSS:PEG molar ratio from 3:1 to 8:1. When the temperature increases up to 130 °C, the value of tan δ increases steeply, and the corresponding modulus drops down, indicating the whole sample begins to melt and flow as the crystals of the POSS-rich phase melt.

By comparison with the typical DSC heating curve, also plotted in Figure 4, these mechanical property transitions in DMA analysis are in a good agreement with the corresponding phase transition observed; i.e., the samples become fluidlike when POSS crystalline domains start to melt. Below the glass transition temperature, the tensile storage modulus features an interesting dependence on molar ratio of POSS to PEG. With the molar ratio of POSS to PEG (10 kg/mol) increasing from 3:1 to 6:1, the tensile storage modulus

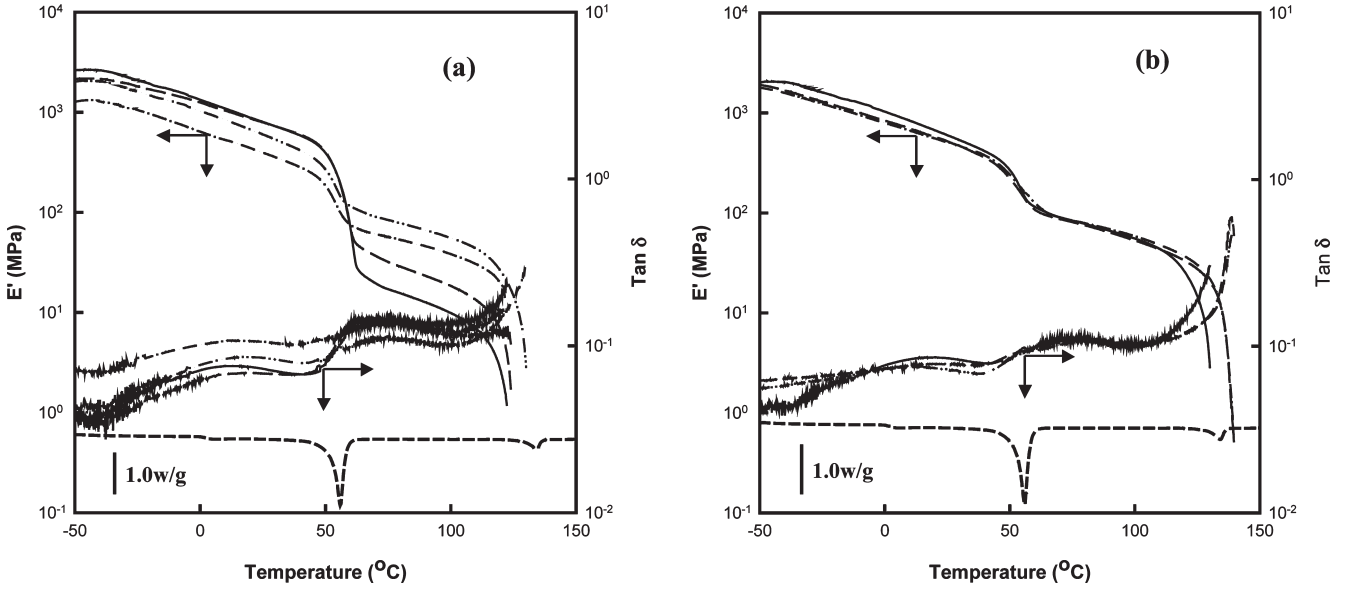

Figure 4. Dynamic mechanical analysis (DMA). (a) Varying POSS:PEG mole ratio at fixed PEG mol wt of 10 kg/mol (3:1 —); (4:1 − − −); (6:1 —·—·); (8:1 —··—··). (b) Varying PEG molecular weight with POSS loading level fixed at 50 wt %: (10 kg/mol —); (20 kg/mol − − −); (35 kg/mol —·—·). The DSC heating curve of the PEG(10)$POSS_8$ heated at 10 °C/min is included for reference.

decreases by half from 1.33 to 0.64 GPa at 0 °C. However, when the ratio reaches 8:1, the tensile storage modulus increases back to 1.03 GPa. This trend is the same as that for the latent heat of melting for PEG-segments crystals observed in the DSC experiments. This indicates that, at low temperatures, the tensile storage modulus increases with increase of PEG-segment crystallinity, while any reinforcement from the increase in POSS crystallinity cannot compensate for the modulus *decrease* caused by the loss of PEG crystallinity. Above the melting point of PEG, the tensile modulus for all compositions of this series steps down to values of a stiff rubber, $10 < E' < 100$ MPa, and remains as such until the temperature is increased above the melting point of POSS-segments. This rubbery plateau reflects the physical cross-linking network formed by POSS crystal moieties. As expected, the rubbery plateau modulus decreases with decreasing of POSS:PEG molar ratio.

In contrast to the significant impact of POSS:PEG variation at fixed PEG molecular weight, variation in PEG molecular weight has virtually no impact on thermomechanical behavior of the TPU in rubbery state as long as the POSS wt % is held fixed. Figure 4b shows the dependence of tensile storage modulus and loss tangent on temperature as PEG molecular weight is varied at roughly fixed POSS incorporation level of ca. 50 wt %. Within the glassy state, the tensile storage modulus decreases from modestly from 1.03 to 0.79 GPa (T = 0 °C) with the increase of PEG molecular weight from 10 to 35 kg/mol. This trend is also the same as the dependence of the latent heat of melting for PEG-segments on PEG molecular weight observed with DSC. It further confirms the predominant role of PEG crystals in the modulus within the semicrystalline, glassy state. Above the melting of PEG-segments, the rubbery plateau modulus is almost independent of PEG molecular weight, reflecting the nature of the physical cross-linking network formed by POSS crystal moieties. At such temperatures, the tensile modulus appears to depend only on the POSS-segment crystal content. Although the PEG molecular weights studied are all above their entanglement molecular weight ($M_e \cong 4400$ g/mol), the chain entanglement contribution to the rubbery plateau modulus is apparently minor. Increasing the temperature still further leads to a sudden loss of the rubbery plateau at the melting point, closely tracking with DSC results, and the samples began to flow. On the basis of these data, the hybrid polyurethanes can be characterized as hydrophilic PEG network structures that are physically cross-linked by hydrophobic POSS crystals.

Many commercial polyurethanes feature hard segments built from 4,4′-methylenebis(phenyl isocyanate) (MDI) and 1,4-butanediol (BD), characterized by a melting point that normally exceeds 200 °C. Consequently, a high processing temperature is needed for melt processing—high enough to degrade the PEG soft segments during processing or long-duration characterization experiments. By comparison, the melting temperature of POSS hard segments is only ~130 °C, offering the potential to greatly improve thermal stability above T_m. Meanwhile, the two separated melting points offer a great potential application for shape memory effect based on the PEG T_m[63,64] and hydrogel behavior. Here we turn our attention to water-swelling behavior and hydrogel properties in light of significant interest in such materials for medical applications.

4. Swelling Behavior. The PEG−POSS polyurethanes were observed to swell when emerged in water, the degree of swelling depending sensitively on composition. Pictures of dry and water-swollen hydrid hydrogels are shown in Figure 5a,b. As shown in Figure 5a, with decreasing molar ratio of POSS to PEG at fixed PEG molecular weight, the swollen volume of the resulting hydrogels increases significantly. By comparison, the influence of PEG molecular weight at fixed POSS wt % (50%; Figure 5b) is less dramatic. The hybrid hydrogel produced from PEG with M_w = 20 kg/mol, PEG-(20)$POSS_{16}$ features slightly larger swelling than the other two. In addition, we can see that, qualitatively, the transparency of the hydrogels also depends on POSS content and PEG molecular weight. The PEG(10)$POSS_6$ sample is the most transparent in Figure 5a (sample iii). Meanwhile, the PEG(20)$POSS_{16}$ hydrogel (iv) shows the highest qualitative transparency in the series of samples with 50 wt % POSS. Although an explanation for this trend in transparency eludes us, we are encouraged by the intrinsic tailorability in hydrogel transparency afforded by POSS incorporation level

and PEG molecular weight. Optical clarity, of course, is significant for some medical devices, such as contact lenses. Hydrogels swell when immersed in water, the water molecules diffusing into the sample to hydrate the polar/hydrophilic groups, leading to volumetric network expansion that comes to an equilibrium swelling extent. The equilibrium swelling is determined by a balance between enthalpically favorable water−polymer interaction and the entropic penalty of network chain extension, as described by the Flory−Rehner theory.[65−67] In the present case of thermoplastic, multiblock hydrogels, the PEG blocks are hydrophilic and drive swelling, while hydrophobic POSS domains serve as physical cross-links that limit swelling.

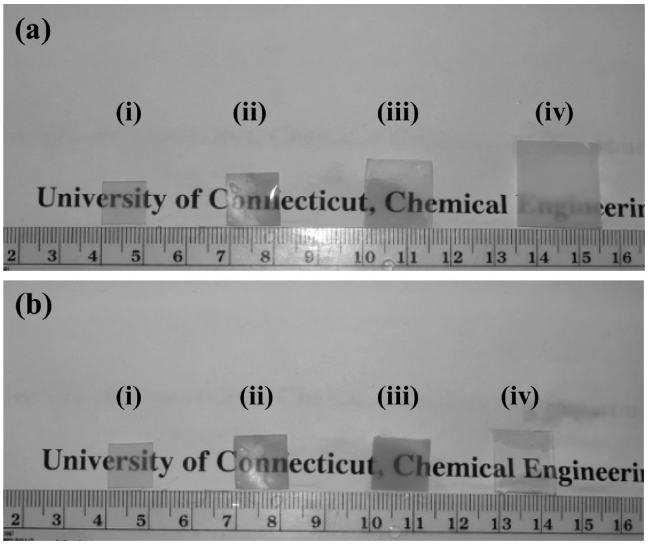

Figure 5. Dry and water-swollen films of the hybrid polyurethanes. (a) Dependence of molar ratio of POSS to PEG: (i) initial dry sample [PEG(10)$POSS_8$], (ii) 8:1, (iii) 6:1, and (iv) 3:1. The molecular weight of PEG homopolymer is 10 kg/mol. (b) Dependence of PEG molecular weight (POSS loading 50 wt %): (i) initial dry sample (PEG(10)$POSS_8$), (ii) 10 kg/mol, (iii) 35 kg/mol, and (iv) 20 kg/mol. The weight fraction of POSS moieties is ~50%. Ruler units are cm.

The internal microstructures of freeze-dried samples of our hybrid hydrogels were examined using SEM (Figure 6), revealing porous microstructures for hydrogel samples PEG(10)$POSS_3$ (Figure 6a) and PEG(10)$POSS_4$ (Figure 6b). Indeed, PEG(10)$POSS_3$ displays a strikingly cocontinuous porous structure. By comparison, PEG(10)$POSS_4$ exhibits a microstructure characterized by isolated pores. When the weight fraction of POSS was increased up to 50 wt %, the porous structure is lost (PEG(10)$POSS_8$, Figure 6c). As we will show momentarily, this observation is associated with a substantially lower swelling degree. Evidently, the more compact network structure for such a sample suppresses the heterogeneity experienced during swelling of water by other samples of lower POSS content. Samples of similarly high POSS content (~50 wt %) but differing PEG molecular weight, for example PEG(20)$POSS_{16}$ and PEG(10)$POSS_8$, featured very similar, homogeneous microstructures (Figure 6, d and c, respectively). This indicates that the hydrogel microstructure is dominated by the POSS loading level, at least at higher POSS levels.

The effect of increasing POSS content on the swelling ratio and kinetics of swelling of the hybrid hydrogels was investigated for all of the samples, first with fixed PEG molecular weight and variable POSS loading and then with fixed POSS loading and variable PEG molecular weight. As shown in Figure 7a, the equilibrium (long time) swelling ratio of the hybrid hydrogels monotonically and dramatically decreases with increasing POSS loading for PEG molecular weight fixed at 10 kg/mol. The decrease in water absorption with increasing POSS loading can be ascribed to the increased interconnectivity of the hydrophobic POSS domains, which increasingly resisted volumetric expansion of the hydrogels by hydration. Figure 7b reveals the complex influence of PEG molecular weight on the swelling ratio for samples

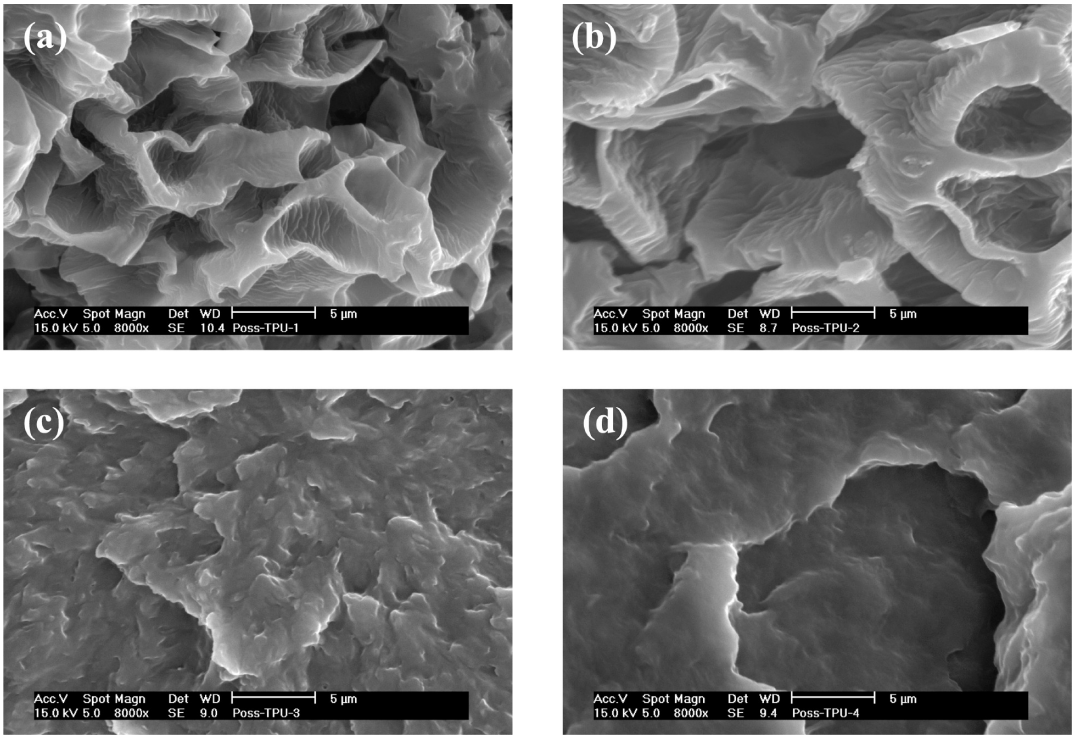

Figure 6. SEM images of the freeze-dried hybrid hydrogels varying in hydrophilic/hydrophobic balance: (a) PEG(10)$POSS_3$, (b) PEG(10)$POSS_4$, (c) PEG(10)$POSS_8$, (d) PEG(20)$POSS_{16}$.

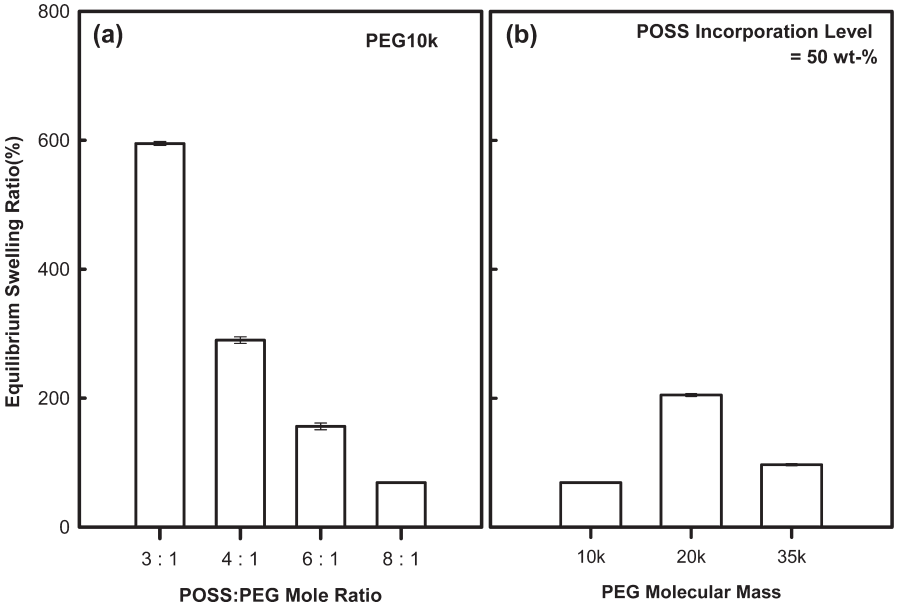

Figure 7. Equilibrium water swelling percentage at room temperature for (a) varying POSS:PEG molar ratio and PEG molecular weight fixed at 10 kg/mol and (b) varying PEG molecular at fixed POSS incorporation level of 50 wt %. Error bars indicate one standard deviation from data sets with sample size $n = 5$.

maintaining a POSS loading of ~50 wt %. Compared with the PEG blocks with 10 and 35 kg/mol, the hybrid hydrogels obtained from PEG of 20 kg/mol feature a higher swelling ratio, which is consistent with the observation of corresponding volume expansion shown in Figure 5b. Nevertheless, a nonmonotonic dependence of swelling on PEG molecular weight eludes explanation.

Water absorption of hydrogels, including absorption kinetics, is of paramount importance to many applications. For example, the rate of drug release and mechanical properties of implanted devices based on the hybrid thermoplastic hydrogels will depend strongly on the rate of hydration and the equilibrium water content. Fundamentally, water uptake may offer insight into the network structure of the hydrogels as well as the resulting transport mechanism of the water absorption process. Generally, the time dependence of water uptake of a polymer can be expressed as follows:[68]

$$F(t) = \frac{m_t - m_d}{m_\infty - m_d} = kt^n \qquad (4)$$

where k is a swelling rate constant related to the structure of the hydrogel network and n is the swelling exponent, which depends on water absorption mechanism. Further, m_d is the mass of dry sample; m_t and m_∞ are the mass of swollen samples at time t and final equilibrium, respectively. As such, $m_t - m_d$ and $m_\infty - m_d$ are the absorbed water mass at time t and the equilibrium, respectively. The transport mechanism of water molecules in the hydrogel depends on polymer chain mobility.[69] If the glass transition (T_g) of the hydrophilic polymer is well below the experimental temperature, the constituent polymer chains exist in a rubbery state and feature a higher mobility. In this case, water absorption will follow Fickian diffusion and the swelling exponent in eq 4, n, will be close to 0.5. For the cases where T_g of the hydrophilic polymer is higher than the experimental temperature, the polymer chains will feature limited mobility so that the polymer chain relaxation rate is lower than water molecule diffusion rate. In such cases, the diffusion will be non-Fickian and the swelling exponent, n, for such cases is between 0.5 and 1.0. The present materials do not match either of these limiting cases due to the nanoscale amphiphilic heterogeneity, coupled with the semicrystalline nature of the hydrophilic phase; our expectations for swelling kinetics were unclear.

Table 3. Water-Swelling Characterization of the Resulting Hybrid Hydrogels

sample	POSS:PEG (feed ratio)	k ($\times 10^3$)	n	S_{eq} (%)
PEG(10)POSS$_3$	3:1	6.32	0.85	599
PEG(10)POSS$_4$	4:1	6.46	0.77	301
PEG(10)POSS$_6$	6:1	6.41	0.63	214
PEG(10)POSS$_8$	8:1	6.85	0.74	69
PEG(20)POSS$_{16}$	16:1	10.91	0.67	203
PEG(35)POSS$_{28}$	28:1	12.16	0.64	99

Figure 8a,b shows a log−log plot of the swelling kinetics $F(t)$ for all of the materials, first for varying POSS content at fixed PEG molecular weight (Figure 8a) and then for fixed POSS content and variable PEG molecular weight (Figure 8b). Generally, the swelling kinetics profiles linearly increase (follow a power law) at the initial stage and then level off when approaching the equilibrium state. The swelling exponent, n, and the swelling rate constant, k, were then estimated from the slope and intercept of the initial swelling stages, the results of which are reported in Table 3. It can be seen that all of the n values are between 0.63 and 0.85, indicating the diffusion of water into the hybrid hydrogels is non-Fickian. We attribute this behavior to the semicrystalline nature of the hydrophilic PEG phase. Although the glass transition of PEG-segments is below the experimental temperature, its melting point is higher than room temperature. Additionally, the rigid POSS phase in nanoscopic proximity to the hydrophilic phase raised the glass transition to be in close proximity to the swelling temperature. Consequently, the hydrophilic polymer chain relaxation may be slower than the diffusion rate of water molecules in the hybrid hydrogels. Close inspection of Figure 8a reveals that the swelling exponent, n, varied in a nonmonotonic fashion with POSS loading level.

As the POSS:PEG ratio increased from from 3:1 to 6:1, the swelling exponent, n, decreases from 0.85 to 0.63 but then increases to 0.74 when the ratio is increased to 8:1. Despite

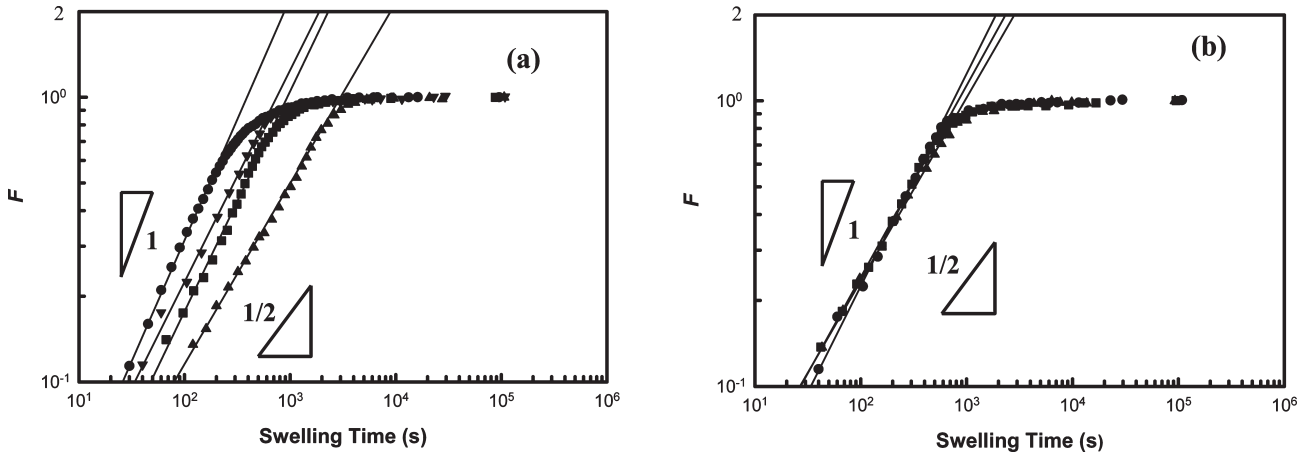

Figure 8. Time dependence of water uptake of the hydrogels produced by the PEG-segmented hybrid polyurethanes in water at room temperature. The molar ratio dependence between POSS and PEG of 10 kg/mol is present in (a): (●) 3:1, (■) 4:1, (▲) 6:1, and (▼) 8:1. The effect of molecular weight of PEG homopolymers is shown in (b), where weight fraction of POSS segment is ~50 wt %: (●) 10 kg/mol, (■) 20 kg/mol, and (▲) 35 kg/mol.

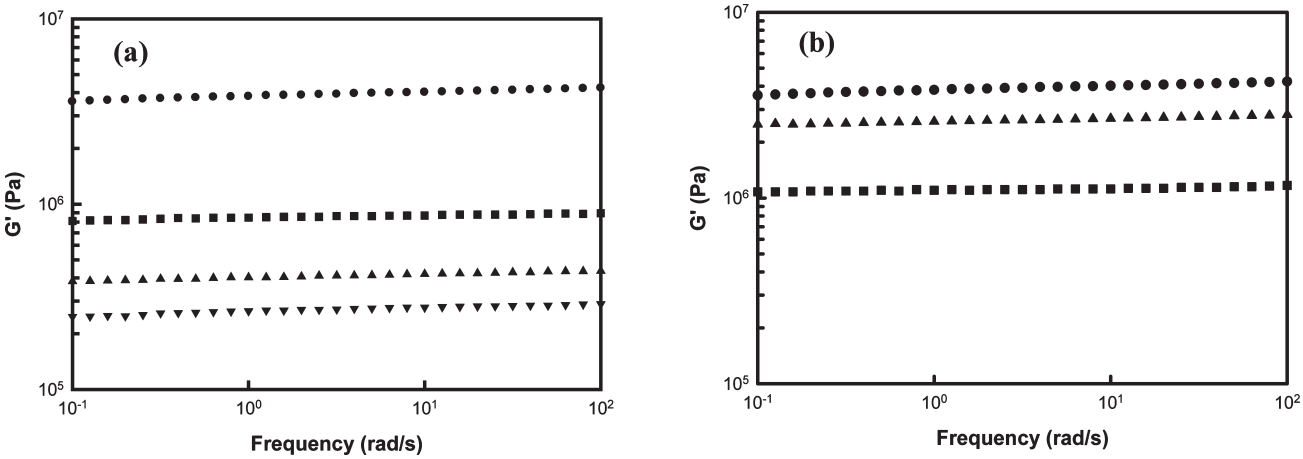

Figure 9. Storage shear moduli (G') as a function of angular frequency (ω) for the hydrogels produced by the PEG-segmented hybrid polyurethanes in water at 25 °C. The molar ratio dependence between POSS and PEG of 10 kg/mol is present in (a): (●) 3:1, (■) 4:1, (▲) 6:1, and (▼) 8:1. The effect of molecular weight of PEG homopolymers is shown in (b), where weight fraction of POSS segment is ~50 wt %: (●) 10 kg/mol, (■) 20 kg/mol, and (▲) 35 kg/mol.

the nonmonotonic behavior, we found positive correlation between the measured swelling exponent, n, and the melting enthalpy of PEG-segments. Specifically, with increasing POSS wt % the latent heat of melting for PEG crystals decreased from 83 to 47 J/g for PEG(10)$POSS_3$ to PEG(10)$POSS_8$, respectively, while the swelling exponent, n, generally decreased for the same range of POSS loadings. In other words, the swelling kinetics became increasingly non-Fickian as PEG crystallinity increased. This phenomenon was not observed for samples with varying PEG molecular weight but constant POSS loading, as shown in Figure 8b. There, we observed that the swelling exponent, n, decreased with molecular weight of PEG, although the latent heat for PEG melting is also roughly constant.

5. Mechanical Properties. The mechanical properties of the new thermoplastic hydrogels at swelling equilibrium were determined in shear using dynamic oscillation rheometry. Figure 9a,b shows log−log plots of the shear modulus as a function of frequency. The dynamic shear storage modulus spectra, $G'(\omega)$, showed frequency invariance. Similarly, the dynamic shear loss modulus spectra, $G''(\omega)$, showed frequency independence (Supporting Information Figure 5). For all samples, G' was at least 10-fold that of G'', indicating elastic behavior. This indicates that the water-swollen, physically cross-linked networks feature minimal dissipation mechanisms, either in the PEG-rich (water-swollen) phase or in the POSS-rich (hydrophobic) phase. The shear storage modulus at 1.0 rad/s increased from 0.26 to 3.8 MPa as the POSS:PEG ratio was increased from 3:1 to 8:1. This demonstrates that the mechanical properties of the hybrid hydrogels can be tuned easily by variation of the hydrophilic−hydrophobic balance. By comparison, the influence of PEG molecular weight on the mechanical properties of the hybrid hydrogels at fixed POSS 50 wt % did not follow a simple trend. The composition with PEG molecular weight of 20 kg/mol (PEG(20)$POSS_{16}$—the most transparent sample) showed a relatively low shear modulus, 1.1 MPa at 1.0 rad/s. Compared to acrylamide-type hydrogels, covalently cross-linked poly(ethylene oxide), or cross-linked alginates with moduli in the 10−100 kPa range, our hybrid thermoplastic hydrogels feature much higher moduli appropriate for load-bearing applications. As such, they may be candidates for orthopedic applications, such as tissue engineered cartilage.[19,23]

Finally, we considered the relationship between swelling degree and shear modulus from a fundamental perspective. Mechanical properties of hydrogels bear a close relationship with hydrophilic polymer network with hydrophobic cross-links. The classic prediction[70,71] for the relationship between these two physical characteristics is

$$G \sim Q_e^{-1/3} \tag{5}$$

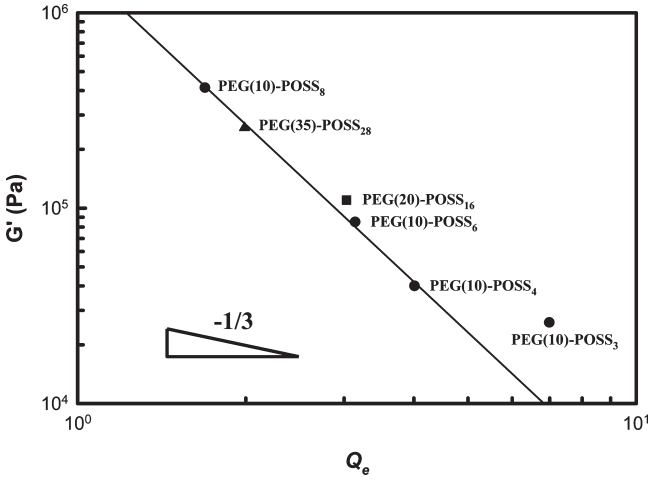

Figure 10. Plot of shear storage moduli (G') vs equilibrium swelling ratio (Q_e) for the hydrogels produced by the PEG-segmented hybrid polyurethanes in water at 25 °C. The molecular weight of PEG varied with (●) 10, (■) 20, and (▲) 35 kg/mol.

where Q_e is defined as the mass ratio of the equilibrated hydrogel to the dry state, $Q_e = (m_\infty/m_d)$. This analysis is based on the assumption that network chains (PEG, in this case) follow Gaussian statistics and that the network deforms affinely. Figure 10 shows a log−log plot of shear storage modulus (G') versus equilibrium swelling mass ratio (Q_e) for all of the hydrogels studied, noting that each point is a different material. Below $Q_e < 4$, the shear storage modulus of the hybrid hydrogels decreases with the increase of equilibrium swelling ratio, according to a power law: $G' \sim Q_e^{-m}$, but with the index being quite large, $m = 2.7$, indicating striking departure from Gaussian behavior. In contrast, the exponent at higher swelling degree ($Q_e > 4$) tends to be close to the value $n = 1/3$ predicted by the classical theory.

We note that the shear modulus obtained from the rheological characterization reflects not only the entropic elasticity of hydrogel but also a reinforcement contribution from the crystalline POSS phase that is geometrically quite far from being pointwise cross-links. Since the POSS weight fraction in our polyurethanes is quite high and in the range 26−50 wt %, it is not surprising that we see departure from classic network theory.

IV. Conclusions

In this paper, we described the synthesis and characterization of the unique hybrid thermoplastic polyurethanes based on hydrophilic poly(ethylene glycol) (PEG) and hydrophobic isobutyl-functionalized POSS-diol. In the dry state, the PEG-rich and POSS-rich blocks independently crystallized, indicating microphase separation. WAXD patterns showed that there are three characteristic diffraction peaks: one of them is attributed to 101 reflection peak of POSS crystals, and the other two are assigned to 120 and $1\bar{3}2$ reflection peaks of PEG. SAXS characterization revealed that the POSS domain microstructure is independent of POSS content (wt %) and molecular weight of PEG and features a characteristic dimension of 2.5−2.7 nm, which is nearly double the diameter of a single POSS molecule, indicating consistency with a raft nanostructure. For dry samples, two melting points appeared and were attributed to PEG (50−60 °C) and POSS (120−135 °C) crystalline domains. The melting point (T_m) and latent heat of melting (ΔH_m) of PEG and POSS each increased with their respective wt % in the hybrid polyurethanes, with one exception being PEG(10)POSS$_8$. At identical POSS incorporation levels, T_m and ΔH_m of the PEG-rich phase increased with PEG block molecular weight. Above the melting point of PEG, the rubbery plateau attributed to the physical cross-linking of POSS crystalline region decreased with POSS loading; however, it was independent of PEG molecular weight for the same POSS loading.

The hybrid polyurethanes absorbed water to form relatively stiff hydrogels. The water absorption of the hybrid hydrogels strongly depended on the POSS:PEG molar ratio and showed independence of PEG molecular weight. As expected, the equilibrium water uptake increased monotonically with PEG wt %. With decreasing POSS:PEG molar ratio (PEG mol wt 10 kg/mol) from 8:1 to 3:1, the swelling ratio dramatically increased from 70% to 600%. The diffusion behavior of water into the hybrid hydrogels was found to be non-Fickian, a finding attributed to PEG crystallinity. Meanwhile, the swelling exponent, n, increased with PEG crystallinity.

At 25 °C, the shear modulus of the hybrid hydrogels increased from 0.26 to 3.8 MPa (1.0 rad/s) with increasing POSS:PEG molar ratio, while there was no dependence of shear modulus on PEG molecular weight at fixed POSS loading. Meanwhile, the transparency of the hybrid hydrogels also has some dependence on POSS incorporation level and PEG molecular weight. Our resulting hybrid hydrogels exist as relatively rigid and transparent materials, though this latter aspect deserves further inquiry. Importantly, the water uptake level, mechanical properties, and transparency of the hydrogels could easily be tuned by the POSS incorporating level and homopolymer PEG molecular weight. It is evident that these hybrid hydrogels with excellent mechanical properties are the good candidates for medical applications, especially those requiring some load-bearing capacity. In addition, the lower melting point of POSS hard segments is expected to be very beneficial for melt processing by allowing such processing safely below the thermal degradation temperature of the PEG soft-block.

In this study, PEG molar mass only spans from 10 to 35 kg/mol. Research examining the impact of PEG molar mass incorporated into such TPUs with a larger range, including below the entanglement molecular weight (< 4.4 kg/mol) and very high molecular weights (> 50 kg/mol)), is expected to achieve a broader spectrum of POSS−PEG TPUs and the resulting hybrid hydrogels. The possible dependence of their physical properties on PEG molar mass will be revealed in more detail and should be pursued in the future.

Acknowledgment. The authors acknowledge support from NYSTAR under a faculty development award, CON01587.

Supporting Information Available: GPC traces, FTIR spectra, NMR spectra, and rheological spectra for selected PEG−POSS multiblock polyurethanes. This material is available free of charge via the Internet at http://pubs.acs.org.

References and Notes

(1) Hoffman, A. S. *Ann. N.Y. Acad. Sci.* **2001**, *944*, 62–73.
(2) Ratner, B. D.; Hoffman, A. S. *Hydrogels for Medical and Related Applications*; American Chemistry Society: Washington, DC, 1976.
(3) Peppas, N. A. *Hydrogels in Medicine and Pharmacy*; CRC Press: Boca Raton, FL, 1987; Vols. *I*−*III*.
(4) Hardland, R. S.; Prud'Homme, R. K. *Polyelectrolyte Gels: Properties, Preparation, and Applications*; American Chemical Society: Washington, DC, 1992.
(5) Hoffman, A. S. Intelligent polymers. In *Controlled Drug Delivery*; American Chemical Society: Washington, DC, 1997.
(6) Loke, W. K.; Lau, S. K.; Yong, L. L.; Khor, E.; Sum, C. K. *J. Biomed. Mater. Res.* **2000**, *53*, 8–17.
(7) Yoshii, F.; Makuuchi, K.; Darwis, D.; Iriawan, T.; Razzak, M. T.; Rosiak, J. M. *Radiat. Phys. Chem.* **1995**, *46*, 169–174.

(8) Franklin, V. J.; Bright, A. M.; Tighe, B. *Trends Polym. Sci.* **1993**, *1*, 9–16.
(9) Sariri, R. *J. Appl. Biomater. Biomech.* **2004**, *2*, 1–19.
(10) Nicolson, P. C.; Vogt, J. *Biomaterials* **2001**, *22*, 3273–3283.
(11) Lee, K. Y.; Mooney, D. J. *Chem. Rev.* **2001**, *101*, 1869–1879.
(12) Hoffman, A. S. *Adv. Drug Delivery Rev.* **2002**, *54*, 3–12.
(13) Drury, J. L.; Mooney, D. J. *Biomaterials* **2003**, *24*, 4337–4351.
(14) Liu Tsang, V.; Bhatia, S. N. *Adv. Drug Delivery Rev.* **2004**, *56*, 1635–1647.
(15) Yeomans, K. *Chem. Rev.* **2000**, *10*, 2–5.
(16) Langer, R.; Vacanti, J. P. *Science* **1993**, *260*, 920–926.
(17) Rowley, J. A.; Madlambayan, G.; Mooney, D. J. *Biomaterials* **1999**, *20*, 45–53.
(18) West, J. L.; Hubbell, J. A. *Macromolecules* **1999**, *32*, 241–244.
(19) Kim, B.-S.; Mooney, D. J. *Trends Biotechnol.* **1998**, *16*, 224–230.
(20) Ito, K. *Polym. J.* **2007**, *39*, 489–499.
(21) Gong, J. P.; Katsuyama, Y.; Kurokawa, T.; Osada, Y. *Adv. Mater.* **2003**, *15*, 1155–1158.
(22) Gong, J. P. *Soft Matter* **2010**, *6*, 2583–2590.
(23) Lee, K. Y.; Rowley, J. A.; Eiselt, P.; Moy, E. M.; Bouhadir, K. H.; Mooney, D. J. *Macromolecules* **2000**, *33*, 4291–4294.
(24) Li, H.; Wang, D. Q.; Liu, B. L.; Gao, L. Z. *Colloids Surf., B* **2004**, *33*, 85–88.
(25) Schiraldi, C.; D'Agostino, A.; Oliva, A.; Flamma, F.; De Rosa, A.; Apicella, A.; Aversa, R.; De Rosa, M. *Biomaterials* **2004**, *25*, 3645–3653.
(26) Azuma, C.; Yasuda, K.; Tanabe, Y.; Taniguro, H.; Kanaya, F.; Nakayama, A.; Che, Y. M.; Gong, J. P.; Osada, Y. *J. Biomed. Mater. Res., Part A* **2006**, *81A*, 373–380.
(27) Yasuda, K.; Gong, J. P.; Katsuyama, Y.; Nakayama, A.; Tanabe, Y.; Konodo, E.; Ueno, M.; Osada, Y. *Biomaterials* **2005**, *26*, 4468–4475.
(28) Petka, W. A.; Harden, J. L.; McGrath, K. P.; Wirtz, D.; Tirrel, D. A. *Science* **1998**, *281*, 389–392.
(29) Mi, L. X.; Fischer, S. E.; Chung, B.; Sundelacruz, S.; Harden, J. L. *Biomacromolecules* **2006**, *7*, 38–47.
(30) Graham, N. B. *Poly*(*ethylene glycol*) *Gels and Drug Delivery*; Plenum: New York, 1992; pp 263−281.
(31) Graham, N. B. *Poly*(*ethylene oxide*) *and Related Hydrogels*; CRC: Boca Raton, FL, 1987; Vol. *2*, pp 95−113.
(32) Hubbell, J. A. *Polym. Prepr.* **1997**, *38*, 528.
(33) Zalipsky, S. *Adv. Drug Delivery Rev.* **1995**, *16*, 157–182.
(34) West, J. L.; Hubbell, J. A. *Biomaterials* **1995**, *16*, 1153–1156.
(35) Ratner, B. D.; Hoffman, A. S. *Hydrogels for Medical and Related Applications*; American Chemistry Society: Washington, DC, 1976; Vol. *31*.
(36) West, J. L.; Hubbell, J. A. *Macromolecules* **1999**, *32*, 241–244.
(37) Cruise, G. M.; Scharp, D. S.; Hubbell, J. A. *Biomaterials* **1998**, *19*, 1287–1294.
(38) Stringer, J. L.; Peppas, N. A. *J. Controlled Release* **1996**, *42*, 195–202.
(39) Salinas, C. N.; Cole, B. B.; Kasko, A. M.; Anseth, K. S. *Tissue Eng.* **2007**, *13*, 1025–1034.
(40) Mathur, A. M.; Hammonds, K. F.; Klier, J.; Scranton, A. B. *J. Controlled Release* **1998**, *54*, 177–184.
(41) Suggs, L. J.; Kao, E. Y.; Palombo, L. L.; Krishnan, R. S.; Widmer, M. S.; Mikos, A. G. *J. Biomater. Sci., Polym. Ed.* **1998**, *9*, 653–666.
(42) Molina, I.; Li, S. M.; Martinez, M. B.; Vert, M. *Biomaterials* **2001**, *22*, 363−369.
(43) Wu, J.; Mather, P. T. *Polym. Rev.* **2009**, *49*, 25–63.
(44) Waddon, A. J.; Zheng, L.; Farris, R. J.; Coughlin, E. B. *Nano Lett.* **2002**, *2*, 1149–1155.
(45) Zheng, L.; Hong, S.; Cardoen, G.; Burgaz, E.; Gido, S. P.; Couglin, E. B. *Macromolecules* **2004**, *37*, 8606–8611.
(46) Kim, B.-S.; Mather, P. T. *Macromolecules* **2002**, *35*, 8378–8384.
(47) Kim, B. S.; Mather, P. T. *Polymer* **2006**, *47*, 6202–6207.
(48) Kim, B. S.; Mather, P. T. *Macromolecules* **2006**, *39*, 9253–9260.
(49) Zeng, K.; Wang, L.; Zheng, S. X. *J. Phys. Chem. B* **2009**, *113*, 11831–11840.
(50) Zhang, W. A.; Muller, A. H. E. *Macromolecules* **2010**, *43*, 3148−3152 .
(51) Wu, J.; Hou, S. Y.; Ren, D. C.; Mather, P. T. *Biomacromolecules* **2009**, *10*, 2686–2693.
(52) Knight, P. T.; Lee, K. M.; Qin, H. H.; Mather, P. T. *Biomacromolecules* **2008**, *9*, 2458–2467.
(53) Wool, R. P. *Polymer Interfaces: Structure and Strength*; Hunser: Munich, 1995; p 102.
(54) Bailey, F. E. J.; Koleske, J. V. *Poly*(*ethylene oxide*); Academic Press: New York, 1976; Chapter IV.
(55) Tadokoro, H.; Chatani, Y.; Yoshihara, T.; Tahara, S.; Murahashi, S. *Makromol. Chem.* **1964**, *73*, 109–127.
(56) Takahashi, Y.; Tadokoro, H. *Macromolecules* **1973**, *6*, 672–675.
(57) Takahashi, Y.; Sumita, I.; Tadokoro, H. *J. Polym. Sci., Polym. Phys. Ed.* **1973**, *11*, 2113–2122.
(58) Waddon, A. J.; Zheng, L.; Farris, R. J.; Coughlin, E. B. *Nano Lett.* **2002**, *2*, 1149–1155.
(59) Zheng, L.; Hong, S.; Cardoen, G.; Burgaz, E.; Gido, S. P.; Coughlin, E. B. *Macromolecules* **2004**, *37*, 8606–8611.
(60) Xu, H. Y.; Kuo, S. W.; Lee, J. S.; Chang, F. C. *Macromolecules* **2002**, *35*, 8788–8793.
(61) Xu, H. B.; Yang, B., H.; Wang, J. F.; Guang, S. Y.; Li, C. *Macromolecules* **2005**, *35*, 10455–10460.
(62) Mark, J. M. *Polymer Data Handbook*; Oxford Univeristy Press: Oxford, UK, 1999.
(63) Jung, Y. C.; So, H. H.; Cho, J. W. *J. Macromol. Sci., Part B: Phys.* **2006**, *45*, 453–461.
(64) Jung, Y. C.; So, H. H.; Cho, J. W. *J. Macromol. Sci., Part B: Phys.* **2006**, *45*, 1189–1189.
(65) Flory, P. J.; Rehner, J. J. *J. Chem. Phys.* **1943**, *11*, 512–520.
(66) Flory, P. J.; Rehner, J. J. *J. Chem. Phys.* **1943**, *11*, 521–526.
(67) Gusler, G. M.; Cohen, Y. *Ind. Eng. Chem. Res.* **1994**, *33*, 2345–2357.
(68) Peppas, N. A. *Pharm. Acta Helv.* **1985**, *60*, 110–111.
(69) Bajpai, A. K.; Shrivastava, M. *J. Appl. Polym. Sci.* **2002**, *85*, 1419–1428.
(70) Treloar, L. R. G. *Physics of Rubber Elasticity*; Clarendon Press: Oxford, UK, 1975.
(71) Flory, P. J. *Principles of Polymer Chemistry*; Cornell University Press: Ithaca, NY, 1978.